

Shifting Adaptation from Weight Space to Memory Space: A Memory-Augmented Agent for Medical Image Segmentation

Bowen Chen¹, Qiaohui Gao², Shaowen Wan³, Shanhui Sun⁴, Wei Liu⁵, Xiang Li⁶, Tianming Liu⁷, and Lin Zhao³

¹ Department of Electrical and Computer Engineering, University of California, Santa Barbara, Santa Barbara, CA 93106, USA

² College of Engineering, Northeastern University, Boston, MA 02115, USA

³ Department of Biomedical Engineering, New Jersey Institute of Technology, Newark, NJ 07102, USA
lin.zhao.1@njit.edu

⁴ United Imaging Intelligence, Burlington, MA 01803, USA

⁵ Department of Radiation Oncology, Mayo Clinic, Scottsdale, AZ 85259, USA

⁶ Department of Radiology, Massachusetts General Hospital and Harvard Medical School, Boston, MA 02115, USA

⁷ School of Computing, University of Georgia, Athens, GA 30602, USA

Abstract. Medical image segmentation is fundamental to clinical workflows, yet models trained on a single dataset often fail to generalize across institutions, scanners, or patient populations. While vision foundation models have shown great promise in addressing this challenge, their deployment typically requires task-specific fine-tuning, which introduces substantial communication overhead in federated learning and prevents continuous knowledge evolution during deployment. In this work, we propose a memory-augmented segmentation agent (MemSeg-Agent) that shifts adaptation from weight space to memory space, enabling few-shot learning, federated supervised learning, and test-time adaptation within a unified architecture. MemSeg-Agent conditions a fixed backbone with lightweight static, few-shot, and test-time working memories, which are dynamically composed by an agentic controller. In federated settings, we update compact memory units instead of model parameters, substantially reducing communication overhead. Experiments on four public datasets demonstrate strong performance and robustness to domain shift: Static memory alone matches or surpasses strong supervised baselines with high parameter efficiency, and test-time working memory further improves in-domain and cross-domain performance without fine-tuning. Overall, MemSeg-Agent introduces a new paradigm for scalable and adaptive medical image segmentation in the era of agentic AI.

Keywords: Agentic Memory · Foundation Models · Federated Learning.

1 Introduction

Medical image segmentation is fundamental to clinical workflows, supporting diagnosis, treatment planning, and intervention guidance [17,2]. Over the past decade, numerous deep learning architectures including CNN-based models [23,10] and transformer-based models [7,9,5] have achieved impressive performance across different modalities [4,16,13]. However, despite the proliferation of increasingly sophisticated models, robust generalization remains unresolved. Models trained on one dataset often experience substantial performance degradation when deployed to new institutions, scanners, or patient populations [21]. This limitation arises from both the inherent heterogeneity of medical images and the limited scale of annotated datasets, which together hinder the learning of domain-invariant representations.

Large-scale vision foundation models have shown potential in reshaping this landscape [20,22,1]. Pretrained on large-scale natural images or multimodal datasets, foundation models learn more transferable feature representations that support robust generalization and adaptation to medical image segmentation tasks such as few-shot segmentation [33] or real-time segmentation [32]. However, most works still require task-specific finetuning of foundation models [26]. Under data privacy constraints, such adaptation becomes challenging to integrate into federated learning (FL) frameworks due to communication overhead even with parameter-efficient fine-tuning (PEFT) [31]. Moreover, the knowledge learned by these models remains largely static after training. Although real-world deployment may provide abundant feedback, there is no efficient mechanism to continuously incorporate them to further adapt the model.

Recent progress on AI agents and agentic memory offers a new promising paradigm [30,3,27]. By decoupling knowledge storage from backbone parameters, a fixed model can operate across heterogeneous contexts while continuously evolving through memory-driven adaptation [6]. Motivated by this, we propose a memory-augmented segmentation agent (MemSeg-Agent) that unifies few-shot learning, federated supervised learning, and test-time adaptation within a single SAM2-based architecture. The agent relies only on lightweight memories (static, few-shot, and test-time working), which are dynamically selected and composed by an agentic controller to condition the backbone. This design also allows maintaining multiple task- or site-specific segmentation priors with only a small memory footprint. In privacy-constrained FL settings, we update supervised static memory instead of model weights, substantially reducing communication overhead. Evaluated on four public datasets, MemSeg-Agent demonstrates strong performance and generalization for domain-shift tasks. We also demonstrate that static memory alone matches or outperforms strong baselines, while test-time working memory further boosts both in-domain and cross-domain performance without fine-tuning.

Our contributions are as follows: (1) We propose a memory-augmented segmentation agent that unifies few-shot learning, federated supervised learning, and test-time adaptation in a single architecture by shifting adaptation from weights to memory. (2) We propose a scalable lightweight supervised memory

that compactly maintains task-/site-specific segmentation priors to plug-and-play condition a fixed backbone, achieving strong performance with minimal additional parameters. (3) We introduce test-time working memory for continual feedback-driven updates, improving both in-domain and cross-domain performance without backbone fine-tuning. (4) We demonstrate communication-efficient federated learning via memory-only updates, reducing per-round communication by $\sim 74.3\times$ ($\sim 98.65\%$) over updating the SAM2-tiny backbone while preserving segmentation accuracy.

2 Related Work

Foundation Models in Medical Image Segmentation. Large-scale foundation models, such as the Segment Anything Model (SAM) [14,22] and DINOv2 [20], have been increasingly adopted for medical image segmentation, demonstrating strong performance and generalization across a range of tasks, including promptable image [18] and video segmentation [19], few-shot learning [33], and real-time segmentation [32]. Instead of relying on parameter-efficient fine-tuning (PEFT), we leverage the memory mechanism to unlock and fully utilize the intrinsic capabilities of these foundation models.

Agentic Memory. Recently, agentic memory systems have enabled LLM-based agents to retain historical interactions, accumulate experiential knowledge, and progressively refine their decision-making processes over time [30]. In the medical domain, emerging efforts have incorporated memory-augmented agents for tasks such as medical question answering (QA) [11] and chest X-ray (CXR) interpretation [8]. However, integrating agentic memory with foundation models for dense prediction tasks remains largely unexplored.

Federated Learning for Foundation Models. Federated learning (FL) has emerged as a critical paradigm for the medical domain, enabling collaborative model training across institutions while preserving data privacy and complying with regulatory constraints [24]. However, when adapting large-scale foundation models in federated settings, existing strategies, ranging from full fine-tuning to PEFT, still incur substantial communication overhead due to the need for frequent synchronization of millions to billions of model parameters across clients. We restrict cross-site updates to lightweight memories, significantly reducing communication costs while preserving strong performance.

3 Methodology

3.1 Overview

We propose a memory-augmented segmentation framework (Fig. 1) built upon a frozen SAM2 backbone [22], where task adaptation is achieved through explicitly parameterized memories, including static memory (Section 3.2), few-shot memory (Section 3.3), and test-time working memory (Section 3.4). An agentic memory controller (Section 3.5) selects memories for inference and regulates the

interaction between static and working memory, enabling efficient adaptation across supervision levels, domain shifts, and distributed settings.

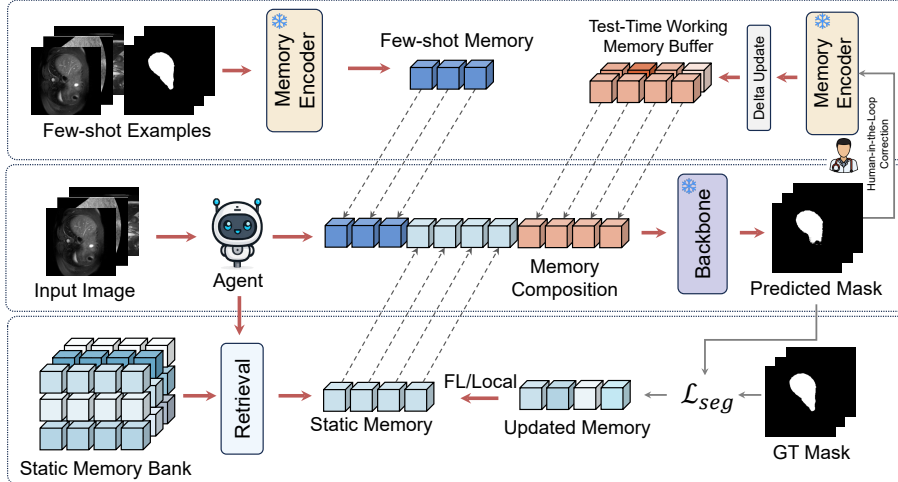


Fig. 1. MemSeg-Agent framework. The agent retrieves and composes static, few-shot, and test-time working memories to condition a frozen backbone for segmentation. Human corrections are encoded into the working-memory buffer via gated delta updates, while static memory can be federated for communication-efficient adaptation.

3.2 Static Memory via Supervision

SAM2’s memory mechanism implicitly defines a representation space $\mathcal{M} \subset \mathbb{R}^d$ that encodes segmentation priors. Given an observation pair (x_i, y_i) consisting of an image frame x_i and its corresponding label or mask y_i , the memory encoder \mathcal{E}_m produces a memory token $\mathbf{m}_i = \mathcal{E}_m(x_i, y_i) \in \mathcal{M}$ that serves as a prior during inference. In this work, we aim to learn a prior \mathbf{m}_i as task-specific static memory that conditions the backbone for downstream segmentation. Directly optimizing \mathbf{m}_i as free parameters in \mathcal{M} discards the observation–encoding regularization and can produce memories that fall outside the \mathcal{E}_m -defined representation manifold. Instead, we optimize parameterized pseudo-observations $\mathbf{z}_i = (\hat{x}_i, \hat{y}_i)$, which are then projected into the memory space via the frozen encoder as $\mathbf{m}_i = \mathcal{E}_m(\hat{x}_i, \hat{y}_i)$. In this way, \mathcal{E}_m acts as an implicit regularizer that constrains the learned static memory to reside within the valid memory representation manifold. To construct static memory, we optimize only the pseudo-observations $\{\mathbf{z}_i\}_{i=1}^N$ while keeping SAM2 backbone f_θ as well as the memory encoder \mathcal{E}_m fixed by solving

$$\min_{\{\mathbf{z}_i\}_{i=1}^N} \mathcal{L}_{\text{seg}}(f_\theta(x; \{\mathcal{E}_m(\mathbf{z}_i)\}_{i=1}^N), y). \quad (1)$$

We perform slice-wise binary segmentation using Dice Loss plus an auxiliary objectness BCE on foreground-presence logits: $\mathcal{L} = \mathcal{L}_{dice}(\hat{y}, y) + 0.3\mathcal{L}_{obj}$.

3.3 Few-shot Memory

When labeled data is scarce, directly learning static memory may overfit. Retrieval-augmented few-shot segmentation [33] can be seamlessly integrated into our framework to support few-shot scenarios. Given a support set $\mathcal{S} = \{(x_i, y_i)\}_{i=1}^K$, we encode each pair into memory $\mathbf{m}_i = \mathcal{E}_m(x_i, y_i) \in \mathcal{M}$ as non-parametric priors. At inference, we retrieve relevant memories by similarity [33] and condition the frozen backbone for the query x_q , i.e., $\hat{y}_q = f_\theta(x_q; \{\mathbf{m}_{i^*}\})$.

3.4 Test-time Working Memory

While static memory encodes stable task priors, it cannot fully handle distribution shifts encountered during inference. When the target domain deviates from the training distribution, relying solely on pre-learned priors may lead to degraded segmentation performance. To address this limitation, we introduce a *test-time working memory* that adapts segmentation priors online during inference. For each test sample x_t , a human-in-the-loop may provide a corrected annotation y_t^* when the model prediction is unsatisfactory. The corrected observation (x_t, y_t^*) is then encoded into memory $\mathbf{m}_t = \mathcal{E}_m(x_t, y_t^*) \in \mathcal{M}$ and written into a working memory buffer $\{\mathbf{m}_j\}_{j=1}^B$ via a gated delta-update strategy [29] to adapt segmentation priors while avoiding uncontrolled memory growth and noisy accumulation. We trigger updates only when $\text{Dice}(y_t^*, y_t) < \tau_{\text{dice}}$, and then compute DINOv3 [25] embedding similarity to existing entries: if $\max_j \text{sim}(\mathbf{m}_t, \mathbf{m}_j) < \tau_{\text{sim}}$, we add \mathbf{m}_t as a new memory; otherwise, we update the matched entry via an exponential moving average (EMA) gated by both similarity and confidence. During inference, top- k working memory entries are retrieved for each query slice and concatenated with static memory to condition the backbone. After inference, working memory entries in the buffer can be persistently stored and reused as domain-specific priors for future inference.

3.5 Agentic Memory Controller

We design an *Agentic Memory Controller* to orchestrate memory usage at inference time. Given a test image, the controller first queries static memory by computing DINOv3 similarity to static prototypes. If a sufficiently similar prototype exists, the agent directly conditions the frozen SAM2 backbone with static memory. Otherwise, the agent requests few-shot examples and encodes them as few-shot memory priors. During deployment, the controller then composes static and working memory to handle domain shift, increasing the working memory contribution and update frequency when similarity to static memory is low. Throughout, the backbone is kept frozen and adaptation is realized solely through memory retrieval, composition, and working-memory updates in the shared SAM2 memory space.

4 Experiments

4.1 Datasets and Preprocessing

We evaluate on three public datasets: **CHAOS** abdominal MRI [12] (kidneys, spleen, liver), **ACDC** cardiac MRI [4] (RV/Myo/LV at ED/ES), and **CAMUS** 2D echocardiography [15] (LV/Myo/LA in 2- and 4-chamber views at ED/ES; ED/ES frames only). For cross-domain testing, we additionally use **CardiacUDA** [28] as an external benchmark (8 patients, 428 slices; CAMUS-matched views). All images are resampled to 0.5×0.5 mm, center-cropped to 256×256 , and intensities are clipped at the top 0.5%. Each dataset is split at the patient level into train/val/test = 3:1:1.

4.2 Implementation Details

All experiments were implemented in PyTorch and conducted on an NVIDIA Blackwell PRO 6000 GPU. Unless otherwise specified, UNet [23], SwinUNETR [9], MedSAM2 [19], and our proposed method were trained for 200 epochs with a batch size of 8. For nnUNet [10], we followed its official configuration and trained for 1000 epochs with a batch size of 2. We used AdamW with a learning rate of 3×10^{-3} and weight decay of 10^{-4} . All experiments regarding our framework were conducted in a slice-wise setting for both training and inference, while evaluation was performed at the 3D volume level by aggregating slice-wise predictions to compute volume-wise metrics.

4.3 Cross-Domain Generalization

We evaluate cross-domain robustness by training on CAMUS and testing directly on CardiacUDA under matched anatomical views. As shown in Table 1, conventional baselines suffer substantial performance drops under domain shift. MedSAM2 shows relatively stronger generalization (42.75% Avg.), likely because it is fine-tuned on large-scale medical data on top of the SAM2 backbone. In contrast, our method keeps the backbone fixed and performs no medical-domain finetuning; nevertheless, the static-only variant reaches 30.74% average Dice and outperforms nnU-Net, SwinUNETR, and U-Net. More importantly, by enabling test-time adaptation through working memory, MemSeg-Agent improves to 77.30% average Dice, a +46.56% absolute gain over static-only and nearly doubling MedSAM2. These results indicate that MemSeg-Agent provides an effective and scalable alternative to parameter updates for cross-domain adaption.

4.4 Evaluation of Static Memory and Test-time Adaptation

We demonstrate the performance of static memory in Table 2 and qualitative results in Fig. 2. Overall, our method achieves performance largely comparable to fully supervised baselines across datasets and supervision levels, frequently attaining best or second-best results in both Dice and HD95, particularly on the

Table 1. Cross-domain evaluation (Train: CAMUS [16], Test: CardiacUDA [28]) on left ventricle (LV) and left atrium (LA). Dice (%).

	nmU-Net [10]	SwinUNETR [9]	U-Net [23]	MedSAM2 [19]	Ours(Static)	Ours(Static+WM)
LV	14.65	33.57	20.30	47.26	39.75	81.53
LA	30.64	0.07	0.03	38.31	21.72	73.07
Avg.	22.65	16.82	10.15	42.75	30.74	77.30

Table 2. Quantitative evaluation of single-class segmentation results under different supervision levels on CHAOS (ABD-MRI), ACDC, and CAMUS.

Sup.	Method	CHAOS (ABD-MRI) [13]								ACDC [4]						CAMUS [16]					
		LK		RK		Spl.		Liv.		RV		Myo		LV		LV		Myo		LA	
		Dice†	HD95‡	Dice†	HD95‡	Dice†	HD95‡	Dice†	HD95‡	Dice†	HD95‡	Dice†	HD95‡	Dice†	HD95‡	Dice†	HD95‡	Dice†	HD95‡	Dice†	HD95‡
100%	U-Net [23]	76.67	43.42	71.37	90.12	67.91	35.03	87.35	13.37	82.03	6.54	86.83	3.05	<u>92.48</u>	4.28	93.36	3.03	86.97	5.00	90.48	4.33
	SwinUNETR [9]	75.34	94.75	80.98	124.78	72.32	111.60	83.15	54.21	71.06	49.87	79.67	51.16	80.69	46.57	93.32	2.91	94.76	1.62	96.32	1.64
	nmU-Net [10]	89.15	14.57	84.91	15.73	82.82	11.36	89.26	10.76	90.53	1.62	90.36	1.12	94.94	1.20	94.61	1.97	<u>89.94</u>	<u>3.01</u>	<u>92.62</u>	<u>3.01</u>
	MedSAM2 [19]	85.42	23.05	87.49	18.90	77.45	37.08	88.65	15.62	<u>87.89</u>	6.27	<u>88.03</u>	<u>1.37</u>	92.05	4.13	<u>93.62</u>	<u>2.31</u>	87.75	4.05	90.30	4.59
	Ours - Static Memory	92.99	3.76	94.10	2.32	88.59	1.95	90.21	3.40	85.26	<u>2.83</u>	84.74	1.78	91.75	2.00	92.66	3.05	85.75	4.96	90.12	4.27
Ours - Static Memory - FL	<u>92.08</u>	3.20	<u>93.14</u>	1.25	90.27	<u>2.60</u>	91.71	2.93	79.54	2.98	83.03	1.70	<u>91.39</u>	<u>1.60</u>	92.34	3.14	85.43	4.97	89.67	4.88	
30%	U-Net [23]	58.33	58.94	61.06	100.93	53.10	59.73	74.10	26.05	75.80	15.21	82.33	4.97	89.63	9.33	92.49	4.03	85.57	6.34	88.98	6.43
	SwinUNETR [9]	44.62	129.70	56.90	138.12	35.50	139.67	65.13	59.24	49.53	71.14	54.90	70.96	69.17	83.78	92.08	4.23	85.11	6.23	<u>89.38</u>	6.01
	nmU-Net [10]	87.69	<u>7.58</u>	<u>86.20</u>	5.72	81.50	<u>17.23</u>	87.41	5.59	87.75	2.87	87.32	2.80	93.37	1.60	93.64	2.52	87.80	3.99	91.61	3.96
	MedSAM2 [19]	44.30	103.71	78.16	42.02	<u>69.15</u>	51.21	82.73	28.37	<u>83.06</u>	11.48	<u>86.17</u>	1.98	<u>91.78</u>	4.12	<u>92.86</u>	<u>3.01</u>	<u>86.29</u>	<u>5.32</u>	89.15	<u>4.48</u>
	Ours - Static Memory	<u>84.32</u>	5.32	86.63	2.74	65.78	6.56	<u>84.55</u>	<u>8.37</u>	78.60	<u>3.27</u>	81.79	<u>2.35</u>	90.70	<u>2.35</u>	91.63	3.85	83.65	6.33	87.30	6.03
10%	U-Net [23]	47.59	88.74	50.74	102.75	21.30	107.76	37.83	63.64	43.20	74.20	64.59	35.93	74.51	39.44	90.87	6.40	83.02	8.86	85.98	11.78
	SwinUNETR [9]	33.07	145.09	31.54	157.03	12.15	134.64	38.79	69.20	50.04	75.02	55.01	73.91	70.40	82.64	90.51	6.25	81.93	9.55	86.73	9.89
	nmU-Net [10]	76.83	<u>32.82</u>	<u>78.10</u>	<u>36.02</u>	68.35	<u>48.02</u>	84.20	<u>28.09</u>	81.72	<u>6.61</u>	83.41	2.60	90.19	3.75	92.88	3.25	86.23	4.93	90.45	5.30
	MedSAM2 [19]	58.96	76.46	70.25	59.99	<u>62.21</u>	81.03	<u>78.83</u>	38.85	<u>79.81</u>	13.54	<u>81.61</u>	<u>3.41</u>	<u>88.20</u>	6.24	<u>91.85</u>	<u>4.12</u>	<u>83.46</u>	8.75	<u>87.57</u>	7.23
	Ours - Static Memory	<u>66.29</u>	10.69	80.10	5.21	56.18	11.17	65.34	15.05	72.71	6.30	78.00	3.72	87.92	<u>5.50</u>	90.38	4.81	81.30	<u>8.24</u>	85.99	<u>7.00</u>

CHAOS (ABD-MRI) dataset, demonstrating the effectiveness of static memory in capturing segmentation priors under limited supervision. In contrast, performance on the CAMUS dataset is relatively modest, likely due to the ambiguous boundaries in ultrasound images, where the edge- and structure-aware features learned by the SAM2 backbone are less transferable; prior work suggests that incorporating semantic cues (e.g., via DINO-based representations) may help mitigate this limitation.

Nevertheless, compared to approaches such as MedSAM2 that require task-specific backbone fine-tuning, our method achieves comparable performance with substantially fewer learnable parameters, enabling scalable plug-and-play deployment without retraining the segmentation model and validating the effectiveness of static memory for encoding segmentation priors. In a simulated four-site FedAvg setting (200 rounds), we update domain priors via memory-only exchange without sharing raw data; updating a 2M-parameter memory instead of the 148.63M SAM2-tiny backbone reduces per-round communication by $\sim 74.3\times$ ($\sim 98.65\%$) while maintaining competitive performance.

To further evaluate the test-time adaptation capability of our framework, we visualize the cross-domain inference process when static memory trained on CHAOS is directly applied to ACDC. As shown in Fig. 3, static memory alone leads to severely degraded performance under distribution shift, whereas enabling the Agent-driven test-time working memory progressively improves segmentation accuracy during inference. This indicates that working memory can dynamically absorb domain-specific information from test samples and compensate for cross-domain discrepancies without updating backbone parameters.

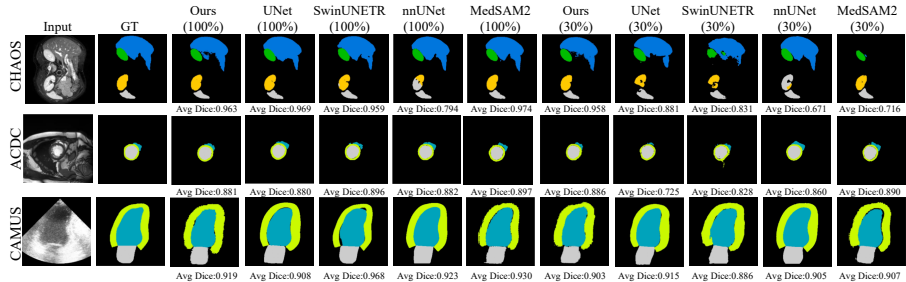


Fig. 2. Qualitative segmentation results on CHAOS, ACDC, and CAMUS under 100% and 30% supervision. Average Dice scores are shown below each prediction.

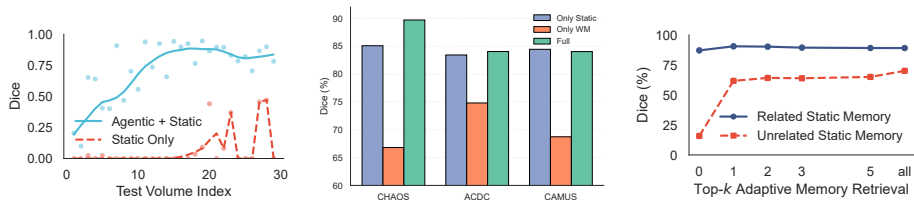


Fig. 3. Test-time Dice progression under cross-domain evaluation (CHAOS \rightarrow ACDC). **Fig. 4.** Ablation study on static and adaptive memory components. **Fig. 5.** Effect of working memory size (Top- k retrieval).

4.5 Ablation Study

We conduct ablation experiments to evaluate the contributions of static and test-time working memory in our framework. As shown in Fig. 4, removing either static or test-time working memory leads to performance degradation across all datasets, with a significantly larger drop observed when only working memory is retained, highlighting the necessity of supervised static priors. We further analyze the effect of test-time working memory size by varying the number of retrieved samples k . As shown in Fig. 5, when static memory is well-aligned with the target distribution (in-domain), performance peaks at small k and gradually degrades with larger memory sizes due to redundant aggregation. In contrast, under cross-domain settings, increasing k consistently improves performance, suggesting that larger working memory capacity facilitates progressive domain adaptation by absorbing target-specific representations.

5 Conclusion

We propose MemSeg-Agent, a SAM2-based segmentation agent that shifts adaptation from weights to lightweight memories, unifying few-shot, federated learn-

ing, and test-time adaptation without finetuning. It improves cross-domain robustness and reduces FL communication by updating compact memory units instead of model parameters, enabling scalable deployment under domain shift and privacy constraints.

References

1. Awais, M., Naseer, M., Khan, S., Anwer, R.M., Cholakkal, H., Shah, M., Yang, M.H., Khan, F.S.: Foundational models defining a new era in vision: A survey and outlook (2023), <https://arxiv.org/abs/2307.13721>
2. Azad, R., Aghdam, E.K., Rauland, A., Jia, Y., Avval, A.H., Bozorgpour, A., Karim-ijafarbigloo, S., Cohen, J.P., Adeli, E., Merhof, D.: Medical image segmentation review: The success of u-net. *IEEE Transactions on Pattern Analysis and Machine Intelligence* (2024)
3. Behrouz, A., Zhong, P., Mirrokni, V.: Titans: Learning to memorize at test time (2024), <https://arxiv.org/abs/2501.00663>
4. Bernard, O., Lalande, A., Zotti, C., Cervenansky, F., Yang, X., Heng, P.A., Cetin, I., Lekadir, K., Camara, O., Ballester, M.A.G., et al.: Deep learning techniques for automatic mri cardiac multi-structures segmentation and diagnosis: is the problem solved? *IEEE transactions on medical imaging* **37**(11), 2514–2525 (2018)
5. Chen, J., et al.: Transunet: Transformers make strong encoders for medical image segmentation. In: *MICCAI* (2021)
6. Chen, Y., Huang, Y., Liu, Y., Zhang, S., He, J., Wu, T., Qi, G., Wu, T.: K-decore: Facilitating knowledge transfer in continual structured knowledge reasoning via knowledge decoupling (2025), <https://arxiv.org/abs/2509.16929>
7. Dosovitskiy, A., et al.: An image is worth 16x16 words: Transformers for image recognition at scale. In: *ICLR* (2021)
8. Fallahpour, A., Ma, J., Munim, A., Lyu, H., Wang, B.: Medrax: Medical reasoning agent for chest x-ray. *arXiv preprint arXiv:2502.02673* (2025)
9. Hatamizadeh, A., Nath, V., Tang, Y., Yang, D., Roth, H., Xu, D.: Swin unetr: Swin transformers for semantic segmentation of brain tumors in mri images. *arXiv preprint arXiv:2201.01266* (2022)
10. Isensee, F., Jaeger, P.F., Kohl, S.A.A., Petersen, J., Maier-Hein, K.H.: nnu-net: a self-configuring method for deep learning-based biomedical image segmentation. *Nature Methods* **18**, 203–211 (2021). <https://doi.org/10.1038/s41592-020-01008-z>
11. Jia, S., Bit, S., Jasodanand, V.H., Liu, Y., Kolachalama, V.B.: Agentic memory-augmented retrieval and evidence grounding for medical question-answering tasks. *International Journal of Medical Informatics* p. 106339 (2026)
12. Kavur, A.E., Gezer, N.S., Barış, M., Aslan, S., Conze, P.H., Groza, V., Pham, D.D., Chatterjee, S., Ernst, P., Özkan, S., et al.: Chaos challenge-combined (ct-mr) healthy abdominal organ segmentation. *Medical image analysis* **69**, 101950 (2021)
13. Kavur, A.E., Selver, M.A., Dicle, O., Barış, M., Gezer, N.S.: CHAOS - Combined (CT-MR) Healthy Abdominal Organ Segmentation Challenge Data (Apr 2019). <https://doi.org/10.5281/zenodo.3362844>, <https://doi.org/10.5281/zenodo.3362844>
14. Kirillov, A., et al.: Segment anything. *Proceedings of the IEEE/CVF International Conference on Computer Vision* (2023)

15. Leclerc, S., Smistad, E., Pedrosa, J., Østvik, A., Cervenansky, F., Espinosa, F., Espeland, T., Berg, E.A.R., Jodoin, P.M., Grenier, T., et al.: Deep learning for segmentation using an open large-scale dataset in 2d echocardiography. *IEEE transactions on medical imaging* **38**(9), 2198–2210 (2019)
16. Leclerc, S., Smistad, E., Pedrosa, J., Østvik, A., Cervenansky, F., Espinosa, F., Espeland, T., Berg, E.A.R., Jodoin, P.M., Grenier, T., Lartizien, C., D’hooge, J., Lovstakken, L., Bernard, O.: Deep learning for segmentation using an open large-scale dataset in 2d echocardiography. *IEEE Transactions on Medical Imaging* **38**(9), 2198–2210 (2019). <https://doi.org/10.1109/TMI.2019.2900516>
17. Litjens, G., et al.: A survey on deep learning in medical image analysis. *Medical Image Analysis* **42**, 60–88 (2017)
18. Ma, J., He, Y., Li, F., Han, L., You, C., Wang, B.: Segment anything in medical images. *Nature communications* **15**(1), 654 (2024)
19. Ma, J., Yang, Z., Kim, S., Chen, B., Baharoon, M., Fallahpour, A., Asakereh, R., Lyu, H., Wang, B.: Medsam2: Segment anything in 3d medical images and videos. *arXiv preprint arXiv:2504.03600* (2025)
20. Oquab, M., Darcet, T., Moutakanni, T., Vo, H., Szafraniec, M., Khalidov, V., Fernandez, P., Haziza, D., Massa, F., El-Nouby, A., et al.: Dinov2: Learning robust visual features without supervision. *arXiv preprint arXiv:2304.07193* (2023)
21. Ovadia, Y., et al.: Can you trust your model’s uncertainty? evaluating predictive uncertainty under dataset shift. In: *NeurIPS* (2019)
22. Ravi, N., Gabeur, V., Hu, Y.T., Hu, R., Ryali, C., Ma, T., Khedr, H., Rädle, R., Rolland, C., Gustafson, L., et al.: Sam 2: Segment anything in images and videos. *arXiv preprint arXiv:2408.00714* (2024)
23. Ronneberger, O., Fischer, P., Brox, T.: U-net: Convolutional networks for biomedical image segmentation. In: *MICCAI* (2015)
24. Sheller, M.J., et al.: Federated learning in medicine: facilitating multi-institutional collaborations without sharing patient data. *Scientific Reports* **10**(1), 12598 (2020)
25. Siméoni, O., Vo, H.V., Seitzer, M., Baldassarre, F., Oquab, M., Jose, C., Khalidov, V., Szafraniec, M., Yi, S., Ramamonjisoa, M., et al.: Dinov3. *arXiv preprint arXiv:2508.10104* (2025)
26. Wang, L., Chen, S., Jiang, L., Pan, S., Cai, R., Yang, S., Yang, F.: Parameter-efficient fine-tuning in large models: A survey of methodologies (2025), <https://arxiv.org/abs/2410.19878>
27. Xu, W., Liang, Z., Mei, K., Gao, H., Tan, J., Zhang, Y.: A-mem: Agentic memory for llm agents (2025), <https://arxiv.org/abs/2502.12110>
28. Yang, J., Ding, X., Zheng, Z., Xu, X., Li, X.: Graphecho: Graph-driven unsupervised domain adaptation for echocardiogram video segmentation (2023), <https://arxiv.org/abs/2309.11145>
29. Yang, S., Kautz, J., Hatamizadeh, A.: Gated delta networks: Improving mamba2 with delta rule. In: *The Thirteenth International Conference on Learning Representations* (2025), <https://openreview.net/forum?id=r8H7xhYPwz>
30. Yu, Y., Yao, L., Xie, Y., Tan, Q., Feng, J., Li, Y., Wu, L.: Agentic memory: Learning unified long-term and short-term memory management for large language model agents (2026), <https://arxiv.org/abs/2601.01885>
31. Zhang, D., Feng, T., Xue, L., Wang, Y., Dong, Y., Tang, J.: Parameter-efficient fine-tuning for foundation models (2025), <https://arxiv.org/abs/2501.13787>
32. Zhang, X., Chen, E.Z., Zhao, L., Chen, X., Liu, Y., Maihe, B., Duncan, J.S., Chen, T., Sun, S.: Adapting vision foundation models for real-time ultrasound image segmentation. In: *International Conference on Medical Image Computing and Computer-Assisted Intervention*. pp. 24–34. Springer (2025)

33. Zhao, L., Chen, X., Chen, E.Z., Liu, Y., Chen, T., Sun, S.: Retrieval-augmented few-shot medical image segmentation with foundation models. *IEEE Transactions on Neural Networks and Learning Systems* (2025)